Physicochem. Probl. Miner. Process. 52(1), 2016, 295−302

www.minproc.pwr.wroc.pl/journal/

Physicochemical Problems of Mineral Processing

ISSN 1643-1049 (print)
ISSN 2084-4735 (online)

Received April 29, 2015; reviewed; accepted June 28, 2015

DEVELOPMENT OF CHARACTERIZATION METHODS FOR ADHERENT ANODE SLIMES IN COPPER ELECTROREFINING

Mikko KIVILUOMA, Miamari AALTONEN, Jari AROMAA, Mari LUNDSTROM, Olof FORSEN

Aalto University, School of Chemical Technology, PO Box 16200, FI-00076 AALTO, Finland, mikko.kiviluoma@aalto.fi

Abstract: Adherent anode slimes can cause anode passivation in copper electrorefining and lower the efficiency of copper electrorefining. Declining concentrate grades cause larger impurity levels in anodes, thus creating larger quantities of slimes in the refining process. In order to investigate the characterization methods for adherent anode slimes in copper electrorefining, experiments were conducted for the Boliden Harjavalta Pori refinery material. Methods such as particle size determination, chemical (ICP) analysis, settling rate determination, XRD, SEM-SE, SEM-BSE and SEM-EDS were applied. In addition, adherent anode slime samples were compared to optical micrograph and SEM-BSE images of respective anode copper samples. It was shown that SEM-EDS and SEM-BSE provided precise information about phases formed during electrorefining. The settling rate and particle size had a correlation only with a copper content of anode slime. The main phases in the anode slime were copper and lead sulphates as well as copper-silver selenides. NiO was shown to be the major Ni-bearing phase in the adherent slime. Nickel, tellurium and lead had the strongest, whereas arsenic, selenium and antimony had the weakest tendency to report to the anode slime.

Keywords: *anode, slime, copper, electrorefining, nickel, lead, arsenic*

Introduction

The dominating trend for all metals refining processes in the 21st century is declining ore grades accompanied by increasing impurity levels. Between 2007 and 2013 there was an increase of roughly 20% in the main impurity elements of copper anodes (Moats et al., 2013). Solid phases in copper electrorefining that originate from anode impurities are referred as slimes. Anode slimes can be classified as adherent, bottom and floating slimes based on their location. These are further divided to primary and secondary slimes based on their formation mechanism (Wang et al., 2011).

http://dx.doi.org/10.5277/ppmp160125

The impurity elements in electrorefining report to either slimes or electrolyte. The major elements reporting to electrolyte are nickel and arsenic, whereas silver, lead, selenium and tellurium report to slimes. The dominant phases in anode slimes are complex oxides, lead sulphate and Ag-Cu selenides (Chen and Dutrizac, 1990). It has been reported that 85% of tellurium in the anode slimes exist in the Cu_2Se-Cu_2Te phase, where tellurium acts as a substitute atom for selenium. The Cu_2Se-Cu_2Te phase is rimming the complex oxide inclusions (Chen and Dutrizac, 1993; 2005). The limit for NiO formation is 0.25% nickel with suitable oxygen concentration and 0.32% nickel with any oxygen level (Forsen, 1985). Nickel may also be found in kupferglimmer, which forms at >0.3% Ni and >200 ppm Sb (Chen and Dutrizac, 1989). The formation methods of bismuth and antimony bearing compounds are not clear in electrorefining (Moats et al., 2012).

For an efficient electrorefining process the following anode slime characteristics are advantageous: (i) adequate adhesion to the surface of anode, but not too firm, (ii) rapidly sinking to the bottom of cell, and (iii) minimum amount of floating particles contaminating cathodes. The objective of this research was to develop a characterization methodology for anode slimes, and moreover to analyze the characteristics and elements excluding PGMs of adherent anode slimes.

Experimental

Adherent anode slime samples were collected from the Boliden Harjavalta's Pori refinery during March-April 2014 from 31 different anode cells, one anode lug and one adherent anode slime sample from each. The adherent anode slimes were collected before washing of anodes, at the end of the electrolysis cycle. Then, the samples were washed with water and filtered at Aalto University. After washing the filtered slime was divided into four sections. One section was dried, one used for particle size analysis and two for settling rate tests. The amount needed to perform all analyses was 50 g. Dried sections were further split into 20 fractions, using a spinning riffler (Microscal L/MSR). The split fractions were combined to create fractions for the chemical, XRD and SEM analyses.

Settling rate testing was done using a 250 cm^3 measuring cylinder and slime to water concentration of 50 g/dm^3. Particle size distribution was done with Malvern Mastersizer 2000, using distilled water as the dispersing agent and ultrasound to break agglomerates. The chemical analysis was done by a certified laboratory - Labtium Oy. A 0.05 g sample was leached at 90 °C with the aqua regia. The volume of the solution was 500 cm^3. After leaching selected elements were analyzed with either inductively coupled plasma mass spectrometry (ICP-MS) or optical emission spectrometry (ICP-OES). Some of the slime samples were also analyzed by Boliden using x-ray fluorescence (XRF). The compounds of all samples were analyzed with a X'Pert PRO PANalytical PW3040/60 x-ray diffractometer. The used slits were FDS (fixed divergence slit, 0.5 mm), FASS (Fixed anti scatter slit, 1.0 mm), AS (automatic slit,

6.4 mm) and brass (15 mm). For SEM analyses about 2 g of dried slime sample was compressed to pellets using 7 megagram pressure. The pellets were further on the cast into epoxy, ground, polished and sputtered with carbon. Anode lugs were cut to 1 cm2 samples, which were also ground and polished. Afterwards they were etched using the ferric chloride solution. The anode samples for SEM were not etched. The SEM used for backscatter electrons (BSE) and energy dispersive spectroscopy (EDS) was LEO model 1450 VP (manufactured by Zeiss, Germany) and Oxford Instruments INCA software. The secondary electron (SE) images were done by using the Tescan Mira 3 GMH microscope. Olympus PMG3 was used as the the optical microscope.

Results

Copper anode

The average anode compositions used in this research are given in Table 1. The anode nickel content varied between 2000 and 5000 ppm. This concentration range favors formation of NiO-particles in anodes, which further report to anode slimes. Also the antimony level was sufficient in every anode to support kupferglimmer formation.

Table 1. Average anode and adherent anode slime chemical compositions of 31 anodes and adherent anode slimes determined by ICP-MS and ICP-OES

	Anode [ppm]	Slime [%]
Ag	1409	21.05
Pb	666	8.35
As	2481	5.40
Sb	492	3.73
Bi	536	5.48
Ni	3071	2.96
Te	249	1.50
Se	606	6.48
O_2	1919	-
Cu	Bal.	17.70

Because of high variation in impurity levels, some distinctive differences were found in an anode microstructure using the combination of optical microscopy and SEM-BSE. Fig. 1 shows dendrites formed during cooling and impurities formed along grain boundaries. The darker areas between the dendrites are the eutectic phase that solidified last. However, the different impurities could not be identified from the optical image in Fig. 1. With the subsequent use of SEM-BSE (Fig. 2), the oxide impurity particles could be identified. The main impurity is Cu_2O that is clearly visible as dark grey areas in Fig. 2, and the other oxide impurities with high molar masses are white. Because NiO has lower molar mass than the copper matrix, it is seen as a dark

phase and can be identified from its crystal shape. Figure 2 also shows that that the oxide-phase (5) solidified between two Cu_2O inclusions and encapsulated them as one. Other phases in the anodes, not visible in Fig. 2, were as following: $Cu_2(Se,Te)$, kupferglimmer and Cu_2O. $Cu_2(Se,Te)$ was present in connection to other phases, kupferglimmer as a separate inclusion and Cu_2O as the most common impurity.

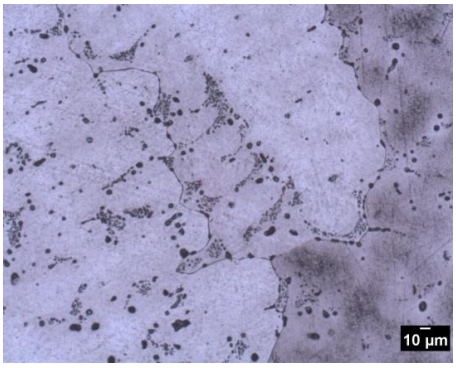

Fig. 1. Anode micrograph, 20x magnification, etched with ferric chloride. Dendrites formed in cooling and impurities at grain boundaries

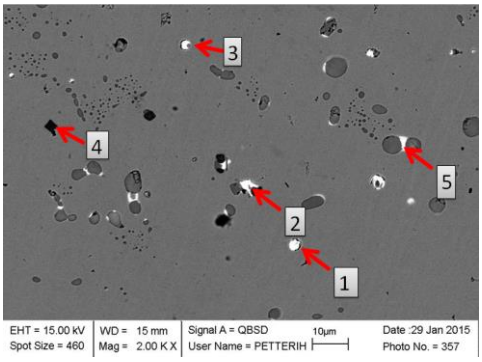

Fig. 2. SEM-BSE image of the same anode as in Fig. 1. (1) and (3) Bi-Pb-As-Sb-Cu oxide, (2) Pb-As-Cu oxide, (4) NiO, (5) Pb-As-Sb-Cu-Ni oxide

Adherent slime chemistry

The correlation between anode composition and anode slime composition was calculated from chemical analyses (Table 2). The strongest correlation was observed between nickel, lead and tellurium contents. This suggests that most of nickel in anode slimes exists as non-soluble NiO as well as lead and tellurium also remain in the adherent slimes. The negative correlation of bismuth suggests that it remains dissolved in the electrolyte.

Table 2. Correlation between anode and adherent anode slime compositions

Ag	0.32	Bi	-0.23
Pb	0.51	Ni	0.72
As	0.18	Te	0.58
Sb	0.16	Se	0.17

There is also some correlation between other elements in anode slimes. Tellurium is present as a substitute atom in selenides. In the present study, the correlation between tellurium and selenium contents in anode slimes is 0.90. Another strong correlation of 0.86 is between bismuth and antimony in the anode slimes. Typical bismuth and antimony bearing compounds in the anode slimes are bismuth bearing antimonates (Moats et al., 2012). The chemical analysis of elements was further supported by the SEM-EDS analysis. The objective was to compare the chemical information given by EDS and chemical analysis. With EDS the high variation of nickel in the anode slimes (0.3-12.5 %) could be explained to be caused by NiO particles in some adherent slimes. From Figure 3 it can be seen that the adherent slime consists of more than 10 different phases and particles of 5-20 μm, with some enclosed phases. The results of EDS analysis are presented in Table 3. The advantage of EDS is opportunity to identify the elements in previously mentioned enclosed phases, such as gold in copper sulphate (3, Fig. 3).

The XRD analysis also showed that $PbSO_4$ is present in every anode slime sample. In addition the analysis confirmed the presence of NiO in the anode slime samples. Every sample with nickel content of >2% contained NiO-particles. The XRD analysis was also capable to identify kupferglimmer, which is challenging to detect from SEM-BSE images.

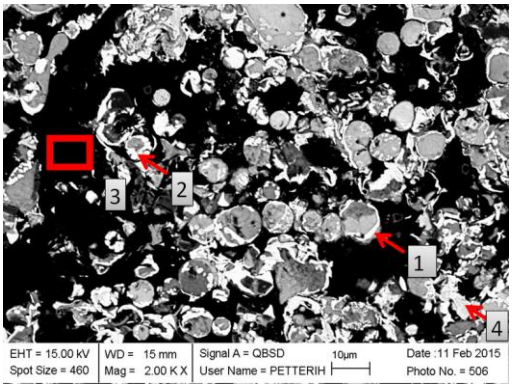

Fig. 3. SEM-BSE image of anode slime sample, (1) and (2) $Ag_2(Se,Te)$, (3) copper oxide - $CuSO_4$, (4) CuAg(Se,Te)

Table 3. EDS-analysis of anode slime sample presented in Fig. 3

Analysis	O	S	Cu	As	Se	Ag	Sb	Te	Au	Pb	Total
1	3.4	0.2	3.4		19.5	62.8		8.1	0.6		98.0
2	8.4	0.8	3.6		17.0	60.6		7.6		4.4	102.4
3	15.4	3.1	47.9	6.7	3.7	5.3	1.3	0.8	2.3		86.5
4	3.9	0.8	12.3	1.0	21.2	48.4		8.1		4.1	99.8

Adherent slime imaging

The main imaging method for adherent anode slimes was SEM-BSE, which was used to determine different phases in the anode slime sample. Some samples were also examined with SEM-SE, in which the overall morphology of sample could be investigated. It was noticed that SEM-BSE is more applicable for characterization, especially with the EDS-detector. It is also noted that the precise use of the BSE-detector for anode slimes benefits from possibility to also use the SE-detector, which is normally found in a SEM-instrument. Figure 4 shows clearly that basing on the SEM-BSE different phases can be found in the anode slimes.

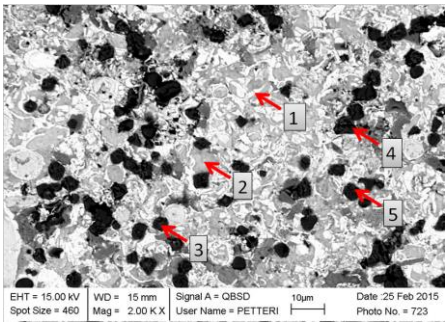

Fig. 4. SEM-BSE image of anode slime sample with NiO-particles.
(1) Cu-As-Sb-Pb –oxide, (2) Cu-As-Pb-Sb –oxide, (3), (4) and (5) NiO

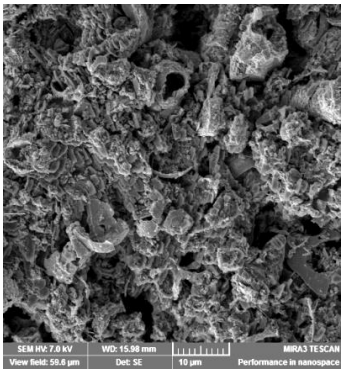

Fig. 5. SEM-SE image of anode slime sample,
which was not ground prior to imaging

Some of the anode slime samples were imaged using SEM-SE without treating the sample surface and an example is shown in Fig. 5. The image shows the slime topography clearly, but does not provide information regarding phase composition.

Adherent slime physical characteristics

An adherent slime was tested for physical characteristics with two different methods: the particle size analysis and settling rate test. The particle size analysis provided quantitative results with $d(0.1)$, $d(0.5)$ and $d(0.9)$ (in μm) and the settling rate test quantitative results in the form of sediment column height. The sediment column heights were further interpreted to three settling rate classes: slow, intermediate and fast. Using 250 mm initial column height, the slimes with fast settling rate reached final height in one minute, intermediate in two and slow in three minutes. From 27 tested slime samples, 11 refereed to have fast settling, 14 intermediate settling and 2 slow settling. The particle size analysis was done for the anode slimes and the average sizes were $d(0.1)$ 3.9±0.6 μm, $d(0.5)$ 13.3±1.6 μm, and $d(0.9)$ 29.7±4.5 μm. The particle sizes were not found to have a clear correlation with the settling rates. The most clear correlation was that the samples with slow settling rate had smaller $d(0.1)$ and $d(0.5)$ particle sizes. The average size of $d(0.1)$ was 9 μm for slow settling, whereas 3.9-4.2 μm for intermediate and fast settlings. The size of $d(0.5)$ was 10.7 μm for intermediate and 13.4-14.2 μm for fast settlings.

From the results it was found, that the increasing copper content of anode slimes correlated positively (0.74) with increasing particle size, especially in particle sizes of $d(0.1)$ and $d(0.5)$. Increasing lead and silver correlated negatively (-0.55), indicating smaller particle sizes. Hence, it was shown, that the chemical composition of adherent anode slime had the effect on the particle sizes. Using the information from the SEM-BSE images, it was shown that the copper sulphate particles were generally larger than lead sulphate and silver selenide particles. The copper content averages for slow, intermediate and fast settling rates were, 8.0±2.1, 15.8±3.9 and 22.5±2.6%, respectively, showing that the copper content has the effect on the settling rate of anode slimes.

Conclusions

Characterization methods for adherent anode slimes were investigated in the current research. It was found that the most informative anode slime characterization for slime behavior in electrorefining is achieved by the chemical analysis of anode slimes supported with settling rate tests, XRD-analysis, SEM-BSE imaging and SEM-EDS analysis. The particle size analysis provided some additional information. Optical microscopy and SEM-SE imaging were not considered to be providing valuable characterization.

The anode lugs and corresponding adherent anode slimes were compared. It was shown that there is a strong correlation between nickel, lead and tellurium in the anode

and anode slime content. The high nickel concentration (> 2%) in anode slimes was shown to consist mostly of NiO-particles.

Particle size analysis showed that the chemical composition of anode slime has the effect on the particle size distribution. The copper content correlated positively with the small particle size. Higher copper content indicated on the large particle sizes $d(0.1)$ and $d(0.5)$, while higher silver and lead compositions indicated on smaller particle sizes. Increasing copper content of anode slime was shown to increase the settling rate of anode slime. The advantageous characteristics of anode slimes for efficient electrorefining were achieved with high copper and low lead and silver contents.

Acknowledgements

This work has been performed within the "*System integrated metals processing*" (SIMP) project coordinated by the Finnish Metals and Engineering Competence Cluster FIMECC Ltd. The authors are grateful for Boliden Harjavalta Copper Refinery for permission to publish the results.

References

CHEN T.T., DUTRIZAC J.E., 1989. *Minerological Characterization of Anode Slimes - IV. Copper-Nickel-Antimony Oxide ("Kupferglimmer") in CCR Anodes and Anode Slimes*. Canadian Metallurgical Quarterly, 28(2), 127-134.

CHEN T.T., DUTRIZAC J.E., 1990. *The Mineralogy of Copper Electrorefining.* Journal of Metals, 42(8), 39-44.

CHEN T.T., DUTRIZAC J.E., 1993. *The Minerological Characterization of Tellurium in Copper Anodes*. Metallurgical Transactions B, 24B, 997-1007.

CHEN T.T., DUTRIZAC J.E., 2005. *Mineralogical characterization of a Copper Anode and the Anode slimes from the La Caridad Copper Refinery of Mexicana de Cobre*, Metallurgical and materials Transactions B, 36B, 229-240

FORSEN O., 1985. *The behaviour of nickel and antimony in oxygen-bearing copper anodes in electrolytic refining.* Doctoral thesis. Helsinki University of Technology. Espoo, Finland.

MOATS M., ROBINSON T., WANG S., FILZWIESER A., SIEGMUND A., DAVENPORT W., 2013. *Global Survey of Copper Electrorefining Operations and Practices*. Abel, R. & Delgado, C. (eds.) Proceedings of Copper 2013, Volume V, Electrowinning / Electrorefining. Santiago, Chile. 307-318.

MOATS M.S., WANG S., KIM D., 2012. *A Review of the Behavior and Deportment of Lead, Bismuth, Antimony and Arsenic in Copper Electrorefining*. Wang, S. & Dutrizac, J. E. & Free, M. L., Hwang, J. Y., Kim, D. (eds.). T. T. Chen Honorary Symposium on Hydrometallurgy, Electrometallurgy and Materials Characterization. Hoboken, New Jersey, USA. 3-21.

WANG X., CHEN Q., YIN Z., WANG M., XIAO B., ZHANG F. 2011. *Homogenous precipitation of As, Sb and Bi impurities in copper electrolyte during electrorefining*. Hydrometallurgy, 105, 355-358.